Int. J. Heat Mass Transfer. Vol. 12, pp. 1123–1139. Pergamon Press 1969. Printed in Great Britain

LAMINAR COMBINED FREE AND FORCED CONVECTION IN VERTICAL NON-CIRCULAR DUCTS UNDER UNIFORM HEAT FLUX

M. IQBAL† and B. D. AGGARWALA‡
University of British Columbia, Canada

and

A. G. FOWLER
Department of Mathematics, University of Calgary, Canada

(*Received* 28 *October* 1968 *and in revised form* 27 *January* 1969)

Abstract—Fully developed laminar combined free and forced convection through vertical non-circular ducts is studied. Geometries treated are (i) right-angled triangle, (ii) isosceles triangle and (iii) rhombic ducts. Uniform axial heat flux and uniform peripheral wall temperature are assumed. All fluid properties are considered constant except for variation of density in the buoyancy terms. Approximate solutions of the problem have been obtained by (i) variational calculus and (ii) finite-difference procedure. For rhombic duct an exact solution for pure forced convection is also presented. For the right-angled triangle the Nusselt number (N_{Nu}) becomes insensitive to the duct angle (α) as the value of the Rayleigh number (N_{Ra}) is increased from zero to about two thousand. As the Rayleigh number is further increased to say ten thousand, the duct angle again becomes important. For the right-angled triangle, at $N_{Ra} = 0$ the maximum value of the Nusselt number is obtained when $\alpha = 45°$, while when $N_{Ra} = 10000$ its minimum value is obtained at $\alpha = 45°$. For the isosceles triangle, the Nusselt number also becomes insensitive to the duct angle as the value of the Rayleigh number is increased from zero to about two thousand. As the Rayleigh number is further increased, to ten thousand, the duct angle again becomes important. For the isoceles triangle, at $N_{Ra} = 0$, maximum value of the Nusselt number is obtained at $\alpha = 60°$ while at $N_{Ra} = 10000$, its maximum value occurs when $\alpha \to 90°$. For the rhombic duct the effect of the duct angle diminishes as the value of the Rayleigh number is increased from zero.

NOMENCLATURE

A, area of cross-section;
A_i, coefficients in the assumed velocity profiles;
a, b characteristic lengths of a duct;
B_i, coefficients in the assumed temperature profiles;
C_p, specific heat of the fluid at constant pressure;
C, a constant;
C_1, temperature gradient in flow direction;
D_h, hydraulic diameter;
E, pressure drop parameter, dimensionless $-\left[D_h^2\left(\frac{\partial p}{\partial z} + \rho_w g\right)\right]/\mu W_m$;
F, heat generation parameter, dimensionless, $Q/\rho C_p C_1 W_m$;
g, gravitational acceleration;
h, average peripheral heat transfer coefficient;
m, tan α for triangular ducts and tan $\alpha/2$ for rhombic duct;
N_{Nu}, Nusselt number, dimensionless, hD_h/k;
N_{Ra}, Rayleigh number, dimensionless, $(\rho^2 g C_p C_1 \beta D_h^4)/k\mu$;
Q, heat generation rate;
q, average surface heat flux;
t, temperature of the fluid;
w, axial velocity;
W_m, mean axial velocity;
W, dimensionless axial velocity, w/W_m;
X, Y, respectively, dimensionless coordinates, x/D_h, y/D_h;
θ, $(t - t_w)$;
T, dimensionless temperature, $\theta\Big/\left(\frac{\rho W_m C_p C_1 D_h^2}{k}\right)$;

† Department of Mechanical Engineering.
‡ Computing Centre.

α, characteristic angle of the duct;

β, ρ, k, μ } fluid properties in standard notation.

INTRODUCTION

THE STUDY of combined free and forced convection in ducts is of particular importance in nuclear power plants, heat exchangers, and many other industrial heat transfer applications. In flow through vertical ducts and channels, many of the combined free and forced convection applications approximate to the case of linearly varying wall temperature boundary conditions. A number of theoretical and experimental investigations are available in this area. Experimental study of laminar flow combined free and forced convection in vertical circular tubes under uniform heat flux has been reported by Brown [1] Hallman [2], Kemeny and Somers [3] among others. Ostroumov [4], Hallman [5], and Morton [6] have presented theoretical studies of the same problem of flow through vertical circular tubes. Ostrach [7] analysed combined free and forced convection of heat generating flows in vertical channels with linearly varying wall temperature.

In laminar combined free and forced convection in vertical circular tubes, the temperature as well as the temperature gradient along circumference remain constant at any tube section. However, in non-circular tubes, the flow is retarded at the corners, thereby carrying away less amount of heat, and increasing the wall temperature in the corners. The extent of rotational asymmetry depends upon the shape of a duct. Under certain circumstances when the wall is sufficiently thick and its thermal conductivity is sufficiently high, the inner peripheral wall temperature may, however, tend to be uniform. In the fully developed region the wall temperature can remain linearly varying in the flow direction, as long as the fluid properties remain constant, except for variation of density in the buoyancy terms, however.

Analytical solutions of flow and heat transfer through noncircular tubes of certain geometries can be borrowed from the results of mathematically analogous differential equations of plate theory. This has been shown by a number of authors, for instance [8]–[10] among others.

Han [11], has analysed combined free and forced convection heat transfer in vertical rectangular tubes by Fourier series analyses. Tao [12], [13] suggests a method of solving such problems by introducing a complex function whose real and imaginary parts are directly related to velocity and temperature fields. By combining the momentum and energy equations, Helmholtz' wave equation in the complex domain is obtained. This equation is then solved in terms of Bessel and associated functions. Agrawal [14] utilized Tao's inhomogeneous Helmholtz' wave equation in complex domain and converted it into an equivalent variational integral. The resulting variational integral was solved by assuming a suitable polynomial for the temperature function.

In this report laminar combined free and forced convection heat transfer in vertical ducts of three shapes; has been studied; (i) right-angled triangular, (ii) isosceles triangular, and (iii) rhombic ducts. Of particular importance is the determination of duct angle which produces maximum value of the Nusselt number, in a manner similar to pure forced convection through triangular ducts [15], [16]. A variational formulation of the problem has been obtained and solved without recourse to complex functions. Results have also been compared with a finite-difference solution, for one of the geometries. An exact solution of pure forced convection through a rhombic duct is also appended.

STATEMENT OF THE PROBLEM AND ASSUMPTIONS

Consider fully developed laminar flow through a straight vertical duct of arbitrary shape as shown in Fig. 1(a). The flow is in the vertical upwards direction along the positive z-axis. Temperature is assumed to vary linearly in the flow direction. The heat flux in the transverse direction is assumed to vary in such a manner

that the wall temperature becomes rotationally symmetric. Viscous dissipation, pressure and axial conduction terms in the energy equation are ignored. The fluid may contain uniform volume heat sources. All fluid properties are assumed constant except for variation of the density in the buoyancy term of the momentum equation.

Under the above conditions, the momentum and energy equations can be written as

$$\mu\nabla^2 w = \frac{\partial p}{\partial z} + \rho g, \tag{1}$$

$$k\nabla^2 t = \rho c_p w \frac{\partial t}{\partial z} - Q, \tag{2}$$

where

$$\nabla^2 \equiv \frac{\partial^2}{\partial x^2} + \frac{\partial^2}{\partial y^2}. \tag{3}$$

The density is assumed to vary linearly with temperature and can be expressed by the relation,

$$\rho = \rho_W[1 - (t - t_W)\beta], \tag{4}$$

where β is the coefficient of thermal expansion of the fluid, and the subscript W refers to the wall conditions. The wall temperature is given by the relation,

$$t_W = t_0 + z\frac{\partial t}{\partial z}, \tag{5}$$

where t_0 is the reference temperature at $z = 0$ and $\partial t/\partial z$ is the constant temperature gradient in the axial flow direction. When equation (4) is inserted in (1), the resultant expression can be written as

$$\mu\nabla^2 w = \left(\frac{\partial p}{\partial z} + \rho_W g\right) - \rho_W \beta g\theta, \tag{6}$$

where the temperature difference function θ is defined as,

$$\theta = t - t_W.$$

The expressions (1) and (2) can now be written in a dimensionless form as,

$$\nabla_1^2 W + N_{Ra} T = -E, \tag{7}$$

$$\nabla_1^2 T - W = -F, \tag{8}$$

where

$$\nabla_1^2 \equiv \frac{\partial^2}{\partial X^2} + \frac{\partial^2}{\partial Y^2}.$$

In (7) and (8), N_{Ra} and F are prescribed parameters, W and T are dependent variables while E is an unknown constant. We therefore require an additional equation which is provided by the continuity considerations

$$\iint W \mathrm{d}A = \iint \mathrm{d}A. \tag{9}$$

The boundary condition at the walls in equations (7), (8) is

$$T = W = 0. \tag{10}$$

An exact analytical solution of equations (7)–(10) for the three geometries (i) right-angled triangle, (ii) isosceles triangle and (iii) rhombic ducts of arbitary angles appears to be very difficult. In the following sections we present a variational formulation of the problem, while the finite-difference procedure is given in Appendix A. Also an exact solution of pure forced convection for the rhombic duct is presented in Appendix B.

VARIATIONAL FORMULATION AND SOLUTION

Consider the expression

$$I = \iint \bar{F}(X, Y, f, \bar{g}, f_x, \bar{g}_x, f_y, \bar{g}_y)\,\mathrm{d}x\mathrm{d}y, \tag{11}$$

where $\bar{F}$ is a given function of the variables $X, Y, f, \bar{g}, f_x, \bar{g}_x, f_y$ and $\bar{g}_y$. The variables f and $\bar{g}$ are supposed to be functions of X and Y; also $f_x = \partial f/\partial x$ etc. The integration is performed over the area of the duct.

For given $\bar{F}$, we obtain different values of I by substituting different functions f and $\bar{g}$ in the right hand side of (11). We are interested only in those functions which vanish on the

boundary of the duct and are differentiable sufficient number of times inside the rhombus. We call such functions "admissible".

Let us assume that there is a pair of admissible functions W and T say, which make I stationary. Now we investigate the value of I in "the neighbourhood" of $f = W$, $\bar{g} = T$. We substitute $f = W + \varepsilon_1 \overline{W}$, $\bar{g} = T + \varepsilon_2 \overline{T}$ where ε_1 and ε_2 are "small" real constants and $\overline{W}$ and $\overline{T}$ are any two admissible functions. For given $\overline{W}$ and $\overline{T}$ we should have

$$\left[\frac{\partial I}{\partial \varepsilon_1}\right]_{\varepsilon_1=\varepsilon_2=0} = 0 \tag{12}$$

$$\left[\frac{\partial I}{\partial \varepsilon_2}\right]_{\varepsilon_1=\varepsilon_2=0} = 0. \tag{13}$$

The equation (11) now becomes

$$I = \iint \bar{F}(X, Y, W + \varepsilon_1 \overline{W}, T + \varepsilon_2 \overline{T}, \overline{W}_x + \varepsilon_1 \overline{W}_x, T_x + \varepsilon_2 \overline{T}_x, W_y + \varepsilon_1 \overline{W}_y + T_y + \varepsilon_2 \overline{T}_y)\, dX dy. \tag{14}$$

By applying the conditions of equations (12), (13), we obtain,

$$\left(\frac{\partial I}{\partial \varepsilon_1}\right)_{\varepsilon_1=\varepsilon_2=0} = \iint \left(\frac{\partial \bar{F}}{\partial W}\overline{W} + \frac{\partial \bar{F}}{\partial W_x}\overline{W}_x + \frac{\partial \bar{F}}{\partial W_y}\overline{W}_y\right) dX dY = 0, \tag{15}$$

$$\left(\frac{\partial I}{\partial \varepsilon_2}\right)_{\varepsilon_1=\varepsilon_2=0} = \iint \left(\frac{\partial \bar{F}}{\partial T}\overline{T} + \frac{\partial \bar{F}}{\partial T_x}\overline{T}_x + \frac{\partial \bar{F}}{\partial T_y}\overline{T}_y\right) dX dY = 0. \tag{16}$$

where $\partial \bar{F}/\partial W$ denotes $\partial \bar{F}/\partial f$ calculated at the "point" $(X, Y, W, T, W_x, T_x, W_y, T_y)$.

Applying Green's theorem to equation (15), we obtain,

$$\iint \overline{W}\left[\frac{\partial \bar{F}}{\partial W} - \frac{\partial}{\partial X}\left(\frac{\partial \bar{F}}{\partial W_x}\right) - \frac{\partial}{\partial Y}\left(\frac{\partial \bar{F}}{\partial W_y}\right)\right] dX dY = 0. \tag{17}$$

Since (17) must hold for all admissible functions $\overline{W}$, we must have

$$\frac{\partial \bar{F}}{\partial W} - \frac{\partial}{\partial X}\left(\frac{\partial \bar{F}}{\partial W_x}\right) - \frac{\partial}{\partial Y}\left(\frac{\partial \bar{F}}{\partial W_y}\right) = 0 \tag{18}$$

inside the duct. Similarly, we obtain.

$$\frac{\partial \bar{F}}{\partial T} - \frac{\partial}{\partial X}\left(\frac{\partial \bar{F}}{\partial T_x}\right) - \frac{\partial}{\partial Y}\left(\frac{\partial \bar{F}}{\partial T_y}\right) = 0 \tag{19}$$

inside the duct. While on the boundary of the duct we will have the condition, $W = T = 0$.

We are interested in solving equations (7), (8) which are rewritten here as,

$$\frac{\partial}{\partial X}\left(\frac{\partial W}{\partial X}\right) + \frac{\partial}{\partial Y}\left(\frac{\partial W}{\partial Y}\right) + N_{Ra}T + E = 0 \tag{20}$$

and

$$\frac{\partial}{\partial X}\left(\frac{\partial T}{\partial X}\right) + \frac{\partial}{\partial Y}\left(\frac{\partial T}{\partial Y}\right) - W + F = 0 \tag{21}$$

Comparing (18) with (20) we obtain,

$$\frac{\partial \bar{F}}{\partial W} = -N_{Ra}T - E, \tag{22}$$

$$\frac{\partial \bar{F}}{\partial W_x} = W_x \quad \text{and} \quad \frac{\partial \bar{F}}{\partial W_y} = W_y. \tag{23}$$

Therefore

$$\bar{F} = -N_{Ra}TW - EW + \tfrac{1}{2}W_x^2 + \tfrac{1}{2}W_y^2 + G(X, Y, T, T_x, T_y), \tag{24}$$

where $G(X, Y, T, T_x, T_y)$ is the "constant" of integration.

From (24) we obtain,

$$\frac{\partial \bar{F}}{\partial T} = -N_{Ra}W + \frac{\partial G}{\partial T}, \tag{25}$$

$$\frac{\partial \bar{F}}{\partial T_x} = \frac{\partial G}{\partial T_x}, \quad \frac{\partial \bar{F}}{\partial T_y} = \frac{\partial G}{\partial T_y}. \tag{26}$$

We see from (25) that if we want (19) to coincide

with (21), we should write (21) in the form

$$N_{Ra}\frac{\partial}{\partial X}\left(\frac{\partial T}{\partial X}\right) + N_{Ra}\frac{\partial}{\partial Y}\left(\frac{\partial T}{\partial Y}\right) - N_{Ra}W + N_{Ra}F = 0. \quad (21a)$$

Comparing (21a) with (19) we obtain,

$$\frac{\partial \bar{F}}{\partial T} = -N_{Ra}W + N_{Ra}F, \quad (27)$$

$$\frac{\partial \bar{F}}{\partial T_x} = -N_{Ra}T_x = \frac{\partial G}{\partial T_x}, \quad (28)$$

$$\frac{\partial \bar{F}}{\partial T_y} = -N_{Ra}T_y = \frac{\partial G}{\partial T_y}. \quad (29)$$

Comparing (27) with (25), we obtain

$$\frac{\partial G}{\partial T} = N_{Ra}F. \quad (30)$$

From (28)–(30) we obtain,

$$G = N_{Ra}FT - \frac{N_{Ra}}{2}(T_x^2 + T_y^2) + H(X, Y) \quad (31)$$

where $H(X, Y)$ is the "constant" of integration. Combining (31) and (24), we obtain,

$$\bar{F} = \tfrac{1}{2}(W_x^2 + W_y^2) - \frac{N_{Ra}}{2}(T_x^2 + T_y^2) - N_{Ra}TW + N_{Ra}FT - EW + H(X, Y). \quad (32)$$

It is clear from (11) that the presence of $H(X, Y)$ in (31) only adds a constant to I and has no effect on its being stationary under the condition of equation (12). Disregarding $H(X, Y)$ we finally obtain,

$$I = \iint(W_x^2 + W_y^2)\,dX dY - N_{Ra}\iint(T_x^2 + T_y^2) \times dX dY - 2N_{Ra}\iint TW dX dY + 2N_{Ra}F \times \iint T dX dY - 2E\iint W dX dY. \quad (33)$$

Admissible functions W and T which make I stationary are the solutions to our boundary value problem. We now solve the problem for each of the three geometries.

COMPUTATIONAL PROCEDURE FOR VARIATIONAL METHOD

(i) *Right angled triangular duct*

Coordinate system for a right angled triangular duct is shown in Fig. 1(b). Our first point of interest is to find approximate expressions for functions W and T. We assume velocity and temperature expressions as

$$W = f_b \cdot (A_0 + A_1X + A_2Y + A_3X^2 + A_4XY + A_5Y^2 + \ldots) \quad (34)$$

$$T = f_b \cdot (B_0 + B_1X + B_2Y + B_3X^2 + B_4XY + B_5Y^2 + \ldots) \quad (35)$$

where $f_b = 0$ is the equation of the boundary, and it ensures $W = T = 0$ at the wall. To simplify the equation of boundary and the resulting calculations, we may take $b = 1$ [see Fig. 1(b)]. However, since (7) and (8) have been non-dimensionalized by the hydraulic diameter, D_h, therefore the final results will require adjustment by the factor b/D_h. The equation of the boundary can now be written as

$$f_b = XY(Y + mX - 1). \quad (36)$$

The expressions (34), (35) were limited to six arbitrary coefficients each for numerical computations. The accuracy of results has been examined with respect to lesser number of coefficients and their effect is described under Discussion. Restricting (34), (35) in this manner, and substituting in (33) we get

$$I = I(A_0, A_1, A_2, \ldots A_5, B_0, B_1, B_2 \ldots B_5, E). \quad (37)$$

We now minimize I with respect to A's and B's. This gives 12 equations

$$\frac{\partial I}{\partial A_i} = \frac{\partial I}{\partial B_i} = 0, \quad i = 0, 1, 2, \ldots 5. \quad (38)$$

Since E is also unknown, we need another equation. This equation is obtained from the continuity consideration,

$$\iint W dX dY = \iint dX dY. \quad (39)$$

Solution of the thirteen equations (38), (39) completes the solution of the problem.

(ii) *Isosceles triangular duct*

Coordinate system for this shape is shown in Fig. 1(c). The velocity and temperature profiles for this case will be symmetric about x-axis but not about y-axis. We have assumed the expression for velocity and temperature as,

$$W = f_b \cdot (A_0 + A_1 Y + A_2 X^2 + A_3 Y^2 + A_4 X^2 Y + A_5 Y^3), \quad (40)$$

$$T = f_b \cdot (B_0 + B_1 Y + B_2 X^2 + B_3 Y^2 + B_4 X^2 Y + B_5 Y^3). \quad (41)$$

In a similar fashion to the previous case, the equation of the boundary for this shape is

$$f_b = Y(Y - mX - 1)(Y + mX - 1). \quad (42)$$

where perpendicular of the triangle is taken as unity. Determination of the coefficients A_i, B_i and the pressure drop parameter E requires the same procedure as outlined for case (i).

(iii) *Rhombic duct*

Coordinate system for the rhombic duct is given in Fig. 1(d). In view of symmetry of this duct about the coordinate axis, we write the approximate expressions for W and T as,

$$W = f_b \cdot (A_0 + A_1 X^2 + A_2 Y^2 + A_3 X^4 + A_5 X^2 Y^2), \quad (43)$$

$$T = f_b \cdot (B_0 + B_1 X^2 + B_2 Y^2 + B_3 X^4 + B_4 Y^4 + B_5 X^2 Y^2). \quad (44)$$

By taking half of the vertical axis of the rhombus equal to unity, the equation of the boundary can be written as

$$f_b = (Y + mX - 1)(Y - mX - 1) \times (Y + mX + 1)(Y - mX + 1). \quad (45)$$

The coefficients A_i, B_i and the parameter E are determined in a similar manner as before.

The method described above can be applied to a duct with any number of sides. However, equation (45) indicates that as the number of sides are increased, the equation of the boundary increases correspondingly and hence the calculations become very lengthy.

Nusselt number

Having obtained the velocity and temperature functions, the evaluation of Nusselt number is straight forward.

$$N_{Nu} = \frac{hD_h}{k} = \frac{D_h}{k}\frac{q}{t_W - t_b} = S\frac{1 - F}{T_{mx}}, \quad (46)$$

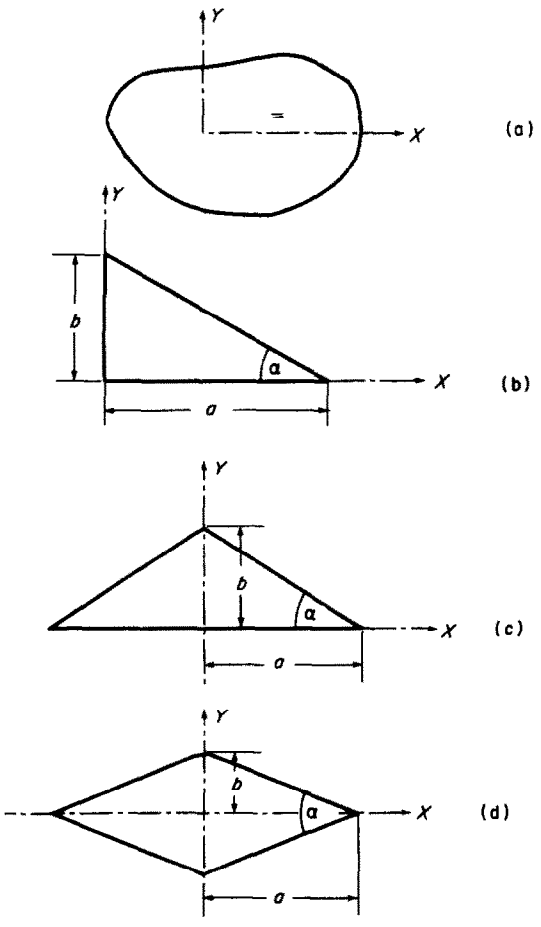

FIG. 1. Coordinate system.

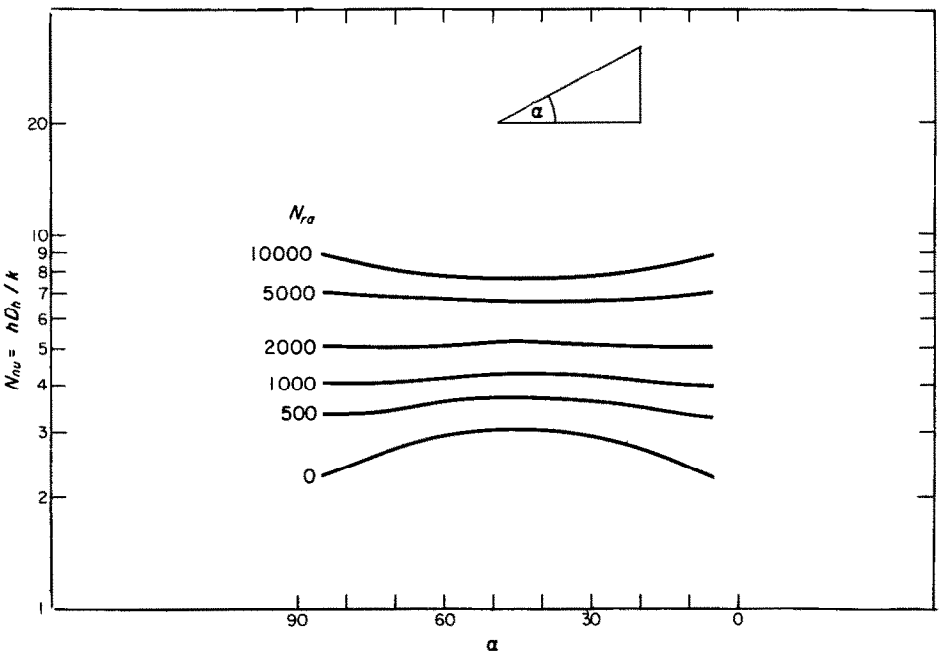

FIG. 2. Nusselt number variation against angle α for various values of the Rayleigh number N_{Ra}.

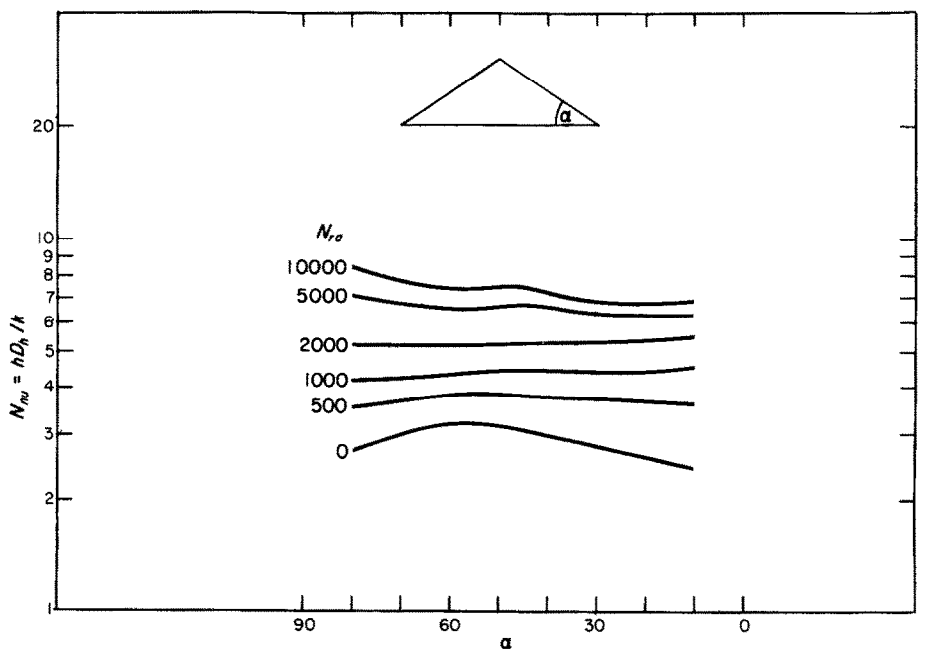

FIG. 3. Nusselt number variation against angle α for various values of the Rayliegh number N_{Ra}.

where T_{mx} is the bulk temperature difference and is given by,

$$T_{mx} = \frac{\int_A TW\,dA}{\int_A W\,dA}, \qquad (47)$$

and S is a factor that depends upon duct geometry.

This completes evaluation of the Nusselt Number.

DISCUSSIONS

We would like first of all to examine the accuracy of the variational results with the results available in the literature wherever it is possible. For pure forced convection through triangular ducts, cases (i) and (ii), the present results given in Figs. 2 and 3 agree with those of [15] and [16]. For the rhombic duct, at $\alpha = 90°$, when it assumes the shape of a square, the present results for combined free and forced convection, Figs. 4, 5, agree with the exact solution presented by Han [11]. For pure forced convection, the present analysis gives Nusselt number of 3·6069 against 3·61 given by Han.

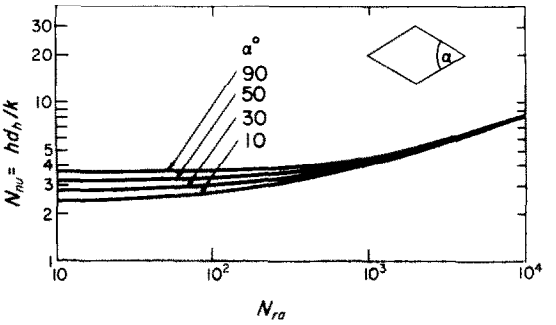

FIG. 5. Nusselt number variation against Rayleigh number N_{Ra} for various values of the angle α.

The comparisons given above are based on six coefficients in the expressions for W and T for each of the three configurations. It was desired to study the manner in which the results are affected by eliminating some of the

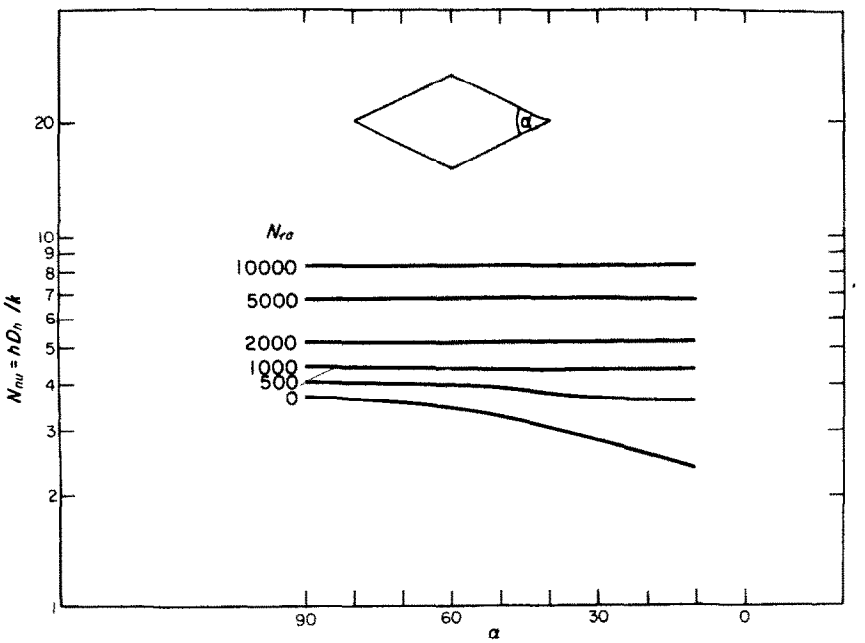

FIG. 4. Nusselt number variation against angle α for various values of the Rayleigh number N_{Ra}.

coefficients in the said expressions. For the right angled triangle, the elimination of XY from (34) and (35) appears to affect the Nusselt number by about five per cent. For the isosceles triangle, elimination of even two terms, containing X^2Y and Y^3 in (40) and (41) affects the Nusselt number by less than five per cent. Still better results are obtained for the rhombic duct. Elimination of two terms containing X^4 and Y^4 from (43) and (44) affects the values of the Nusselt number by less than three per cent. It might be added that the effect on Nusselt number by dropping a term in the expressions for W and T, depends in addition, on the value of the angle α and the value of Rayleigh number for a particular duct. For instance, for triangular ducts, this effect of dropping a term is relatively smaller when α is in the neighbourhood of 45° than when it is in the neighbourhood of 85° or 5°. For rhombic duct, the effect of elimination of two or three coefficients is almost nil at $\alpha = 90°$. It was also noted that while solving equations of the type (38) and (39), the resulting matrices are found to be highly unstable at small values of α. For this reason, in Figs. 2–4 the Nusselt number values are not given for extreme values of α. Also, in general it was found necessary to use double precision in machine calculations, particularly while evaluating the area integrals.

A direct finite-difference solution of equations (8)–(10) was also obtained, primarily to see whether it takes more or less machine time to compute the Nusselt numbers when compared to that of the variational solution. Some

Table 1. Comparison of Nusselt numbers obtained from the finite-difference solutions (Appendix A) with those from the variational solutions, for rhombic duct

$\alpha°$	Nusselt number			
	$N_{Ra} = 0$		$N_{Ra} = 10{,}000$	
	Finite-difference method	Variational method	Finite-difference method	Variational method
90	3·61	3·6069	8·3213	8·3136
80	3·5659	3·5794	8·3192	8·3143
70	3·4884	3·4982	8·3121	8·3159
60	3·3650	3·3665	8·2999	8·3176
50	3·1867	3·1900	8·2845	8·3191
40	2·9692	2·9778	8·2669	8·3210
30	2·7182	2·7465	8·2498	8·3240
20	2·4514	2·5259	8·2354	8·3279

Table 2. Comparison of velocity and temperature at the centre of rhombic duct as obtained for pure forced convection from Appendix B with those from the variational solution

$\alpha°$	90	81	72	63	54	45
			$(W \sin^2 \alpha)/E$			
Appendix B method	0·07368	0·07223	0·06793	0·06109	0·05215	0·04166
Variational method	0·07385	0·07239	0·06811	0·06126	0·05224	0·04165
			$(-T \sin^4 \alpha)/E$			
Appendix B method	0·004063	0·003906	0·003461	0·002806	0·002054	0·001319
Variational method	0·004062	0·003905	0·003462	0·002807	0·002049	0·001309

details of this solution are given in Appendix A. It was observed that the finite-difference solution takes about two hundred times more machine time for every single value of Nusselt number compared to that of the variational solution. Some numerical values of Nusselt numbers obtained by the finite-difference solution for the rhombic duct were compared with those of the variational results and are given in Table 1. This table presents the values of Nusselt number at two extreme values of the Rayleigh number, $N_{Ra} = 0$ and 10 000. As the agreement of the results obtained by these two methods was good and the machine time of the finite difference method was very long, no further attempt was made to compute Nusselt numbers by the finite-difference solution for other geometries. An attempt was also made to compare the variational results with any published exact solution for any of the three geometries. In [17], an exact solution is given for bending of a parallelogram plate. The results of analysis in [17] can be directly utilized for the case of pure forced convection through a rhombic duct. These results are given briefly in Appendix B. A comparison of the numerical values of velocity and temperature at the duct centre as obtained by the exact solution of [17] and the present variational formulation is given in Table 2. This table shows that the results of the variational formulation are indeed very accurate.

We now discuss the general behaviour of the Nusselt number with the variation of α for the three geometries considered. Figure 2 presents the plots of Nusselt number against α for various values of Rayleigh number for the right-angled triangle. The Nusselt number values are symmetric about $\alpha = 45°$. At $N_{Ra} = 0$, (in the present analysis meaning pure forced convection) maximum value of Nusselt number occurs at $\alpha = 45°$. As the value of N_{Ra} is increased from zero, the Nusselt number becomes relatively independent of α. This trend continues until Rayleigh number is in the neighbourhood of about 2000. As the value of Rayleigh number is increased still further, say to 5000 and higher, it appears that the situation is reversed and now minimum value of Nusselt number occurs at $\alpha = 45°$.

For the isosceles triangle, Fig. 3 presents the plots of Nusselt number against α for various values of the Rayleigh number. At $N_{Ra} = 0$, the maximum value of the Nusselt number is obtained at $\alpha = 60°$. As the value of Rayleigh number is increased to the neighbourhood of 2000 the curves flatten out and the Nusselt number becomes relatively insensitive to the variations of α. As the Rayleigh number is increased still further to 5000 and higher values, maximum value of Nusselt number is obtained at $\alpha \to 90°$. For this particular geometry, for $N_{Ra} > 5000$, for some unknown reasons a local maxima of Nusselt number appears to occur at 45°.

Figure 4 presents plots of Nusselt number against α for rhombic duct. For this geometry, at $N_{Ra} = 0$, the maximum value of Nusselt number occurs at $\alpha = 90°$. As the value of α is reduced, the Nusselt number decreases accordingly. As value of the Rayleigh number is increased, the Nusselt number becomes insensitive to the variations in α. This trend continues to the maximum value of the Rayleigh number investigated in this analysis.

Figure 5 shows plots of Nusselt number against Rayleigh number for various values of α for the rhombic duct. This plot also shows that as the Rayleigh number value is increased, the differences between the Nusselt numbers for various values of the included angle α diminishes for this geometry.

Hydraulic diameter is almost invariable used as a characteristic length dimension evaluating the Nusselt number. For turbulent flow through non-circular ducts, hydraulic diameter is known to correlate the pressure drop and heat transfer phenomena. In laminar flow through non-circular ducts, hydraulic diameter is not sufficient to remove the dependence of the heat transfer results upon geometric parameters. As such, for one of the geometries, we have also computed the Nusselt numbers based on a length dimen-

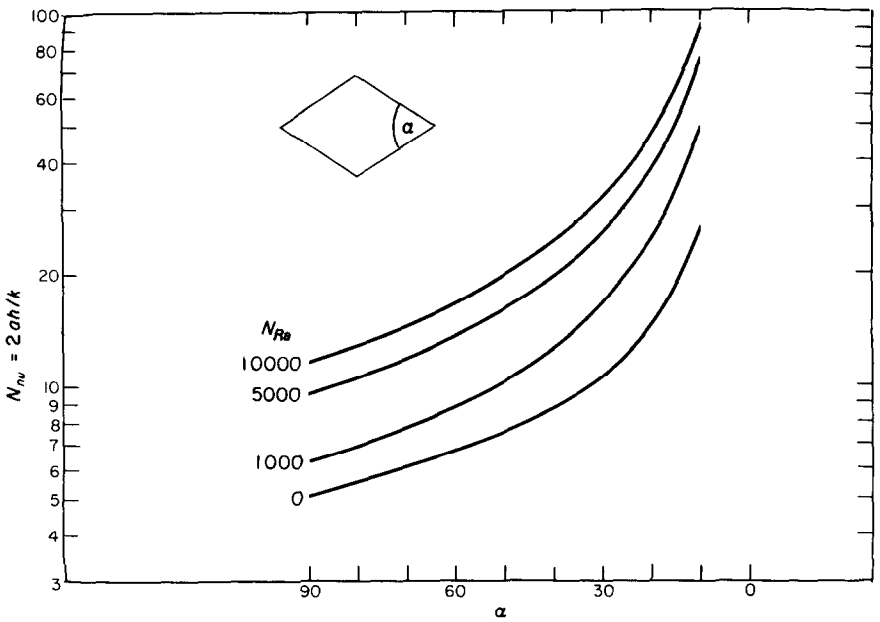

FIG. 6. Nusselt number $N_{Nu} = 2ah/k$ based on the major axis.

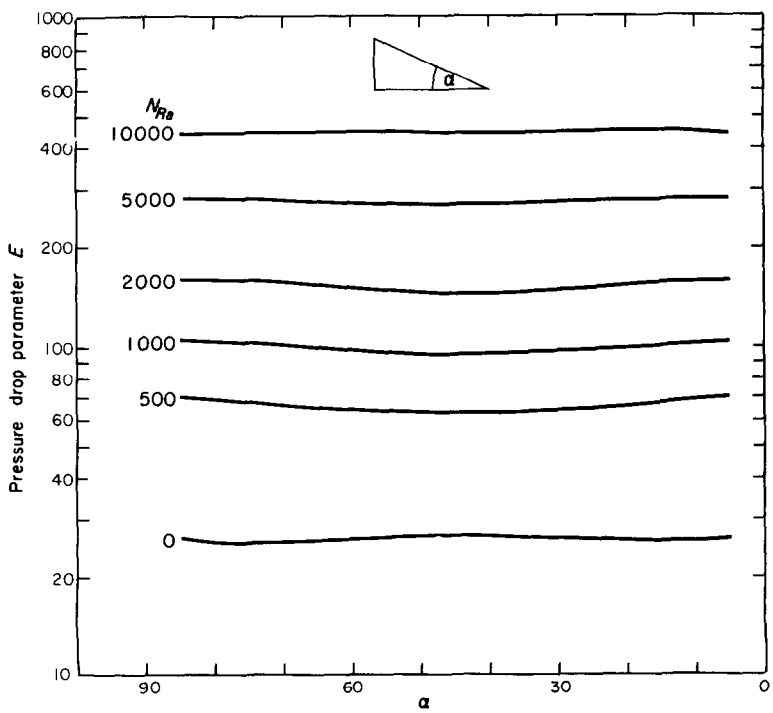

FIG. 7. Pressure drop parameter E variation against angle α for various values of the Rayleigh number N_{Ra}.

sion other than the hydraulic diameter. The case treated is that of rhombus where the Nusselt number is based on the major axis, $2a$. These plots of Nusselt number based on $2a$ are presented in Fig. 6. This figure shows that the geometric factors involved in the selection of a characteristic length dimension may show a completely different trend for Nusselt number based on hydraulic diameter (Fig. 4) when compared to the Nusselt numbers based on $2a$ (Fig. 6). The remarks made above are purely to illustrate a fact that the Nusselt number values and the manner in which they will vary with α will depend also on the characteristic length dimension employed in the Nusselt number itself. A similar observation has been reported by Sparrow *et al.* ([18], Fig. 3), for instance.

The plots for pressure drop parameter E are given in Fig. 7–9. All the three plots indicate that as the value of Rayleigh number is increased from zero, the pressure drop parameter becomes insensitive to the variations in α. In addition, the values of the pressure drop parameter are about the same for all the three ducts, under the same value of the Rayleigh number.

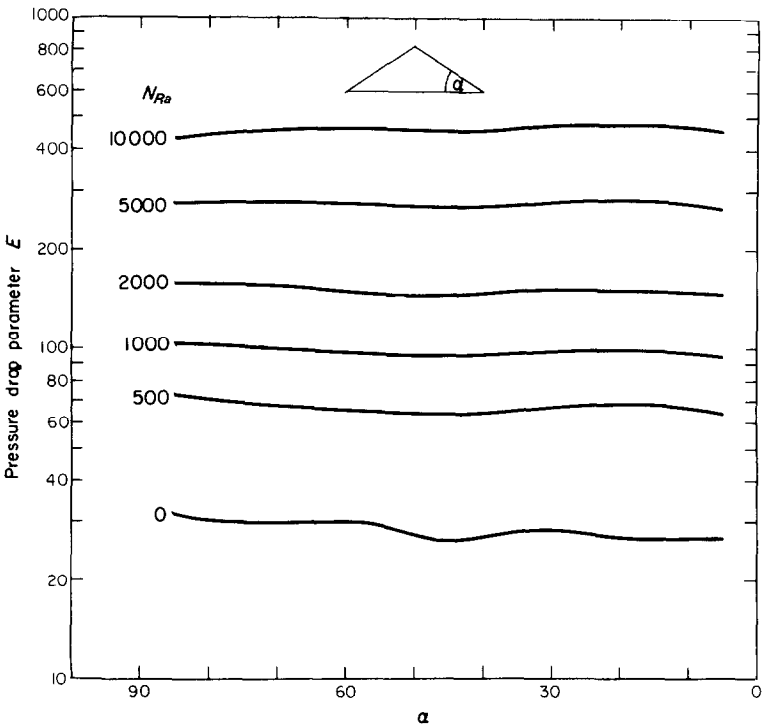

FIG. 8. Pressure drop parameter E variation against angle α for various values of the Rayleigh number N_{Ra}.

Velocity and temperature profiles were examined. Of particular interest was the behaviour of the velocity profiles with variations of the free convection effects and the duct angle. It is known that for heating in upflow, the lower density fluid near the walls accelerates upwards. To satisfy continuity, the flow slows down at the duct 'centre'. If the buoyancy effects are large enough, it is possible to obtain flow reversal at the duct centre, while the net flow remains

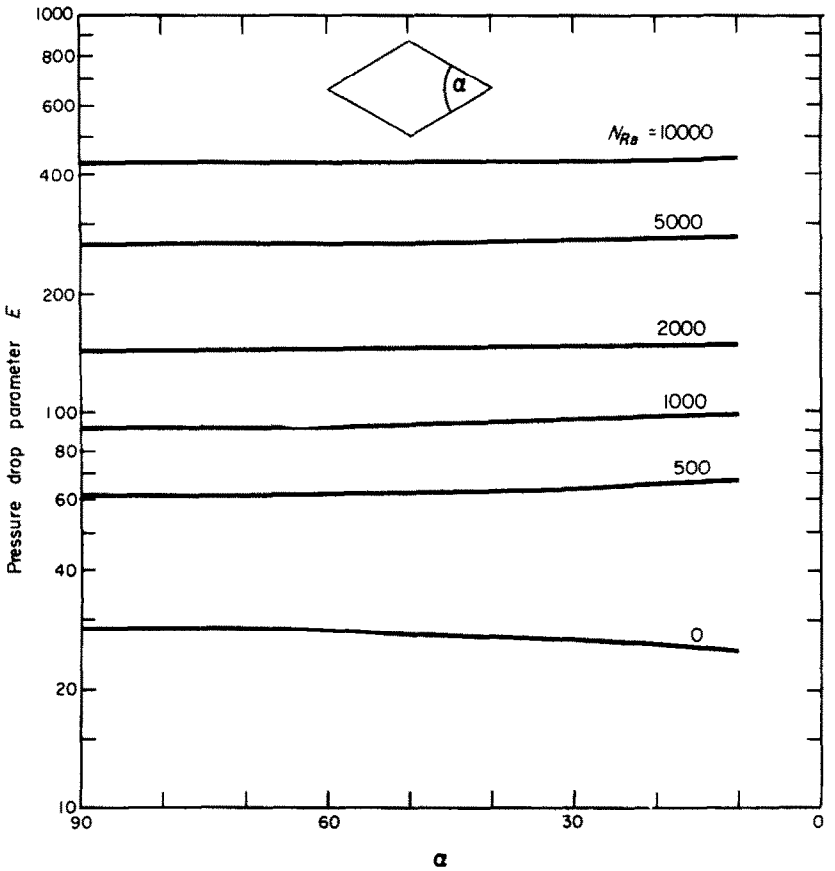

FIG. 9. Pressure drop parameter E variation against angle α for various values of the Rayleigh number N_{Ra}.

in the upwards direction. This study shows that for all the three ducts, the flow reversal occurs when the Rayleigh number is in the range of 10 000. The duct angle α has only a minor effect on the flow reversal.

CONCLUSIONS

Combined free and forced convection through vertical non-circular ducts has been analysed by a variational solution. Three geometries have been treated (i) right-angled triangle (ii) isosceles triangle and (iii) rhombic duct. For particular cases the results of the present analysis agreed with those of the published literature. The Nusselt number variation with the characteristic duct angle depends upon the value of the Rayleigh number. The pressure drop parameter for all the ducts becomes independent of the angle α at higher Rayleigh numbers.

ACKNOWLEDGEMENTS

We would like to thank Mr. Ansari for his devoted help in computing the numerical work involved with the variational solution, Miss Carolyn Moore and Mr. Madderom for assistance in the finite-difference solution of the problem. Financial assistance provided by the National Research Council of Canada and the facilities provided by the Computing Centre of the University of British Columbia are gratefully acknowledged.

REFERENCES

1. W. G. BROWN, Die Uberlagerung von erzwungener und natulicher Konvektion bei niedrigen Durchsatzen in einum lotrechten Roher, *ForscHft. Ver. Dt. Ing.* **26**, 1–31 (1960).
2. T. M. HALLMAN, Experimental study of combined forced and free convection in a vertical tube, NASA Technical Note D-1104, December (1961).
3. G. A. KEMENY and E. V. SOMORS, Combined free and forced-convection flow in a vertical circular tube—experiments with water and oil, *Trans. Am. Soc. Mech. Engrs* (C), *J. Heat Transfer* **84**, 339–346 (1962).
4. G. A. OSTROUMOV, Mathematical theory of the steady heat transfer in a circular vertical hole with superposition of forced and free laminar convection, *J. Tech. Phys.* (In Russian), **20**, 750–757 (1950).
5. T. M. HALLMAN, Combined forced and free laminar heat transfer in vertical tubes with uniform internal heat generation, *Trans. Am. Soc. Mech. Engrs* **78**, 1831–1841 (1956).
6. B. R. MORTON, Laminar convection in uniformly heated vertical pipes, *J. Fluid Mech.* **8**, 227–240 (1960).
7. S. OSTRACH, Combined natural and forced-convection laminar flow and heat transfer of fluids with and without heat sources in channels with linearly varying wall temperatures, NACA TN 3141 (1954).
8. S. M. MARCO and L. S. HAN, A note on limiting laminar Nusselt number in ducts with constant temperature gradient by analogy to thin-plate theory, *Trans. Am. Soc. Mech. Engrs* **77**, 625–630 (1955).
9. E. R. G. ECKERT, T. F. IRVINE, Jr. and J. T. YEN, Local laminar heat transfer in wedge-shaped passages, *Trans. Am. Soc. Mech. Engrs* **80**, 1433–1438 (1958).
10. PAU-CHANG LU, Combined free and forced convection heat-generating laminar flow inside vertical pipes with circular sector cross sections, *Trans. Am. Soc. Mech. Engrs*, (C), *J. Heat Transfer* **82**, 227–232 (1960).
11. L. S. HANS, Laminar heat transfer in rectangular channels, *Trans. Am. Soc. Mech. Engrs* (C), *J. Heat Transfer* 121–128 (1959).
12. L. N. TAO, On combined free and forced convection in channels, *Trans. Am. Soc. Mech. Engrs* (C), *J. Heat Transfer*, **82**, 233–238 (1960).
13. L. N. TAO, Heat transfer of combined free and forced convection in circular and sector tubes, *Appl. Sci. Res.* (A), **9**, 357–368 (1960).
14. H. C. AGRAWAL, Variational method for combined free and forced convection in channels, *Int. J. Heat and Mass Transfer*, **5**, 439–444 (1962).
15. E. M. SPARROW and A. HAJI-SHEIKH, Laminar heat transfer and pressure drop in isosceles triangular, right triangular and circular ducts, *Trans. Am. Soc. Mech. Engrs*, (C), *J. Heat Transfer*, **87**, 426–427 (1965).
16. F. W. SCHMIDT and M. E. NEWELL, Heat transfer in fully developed laminar flow through rectangular and isosceles triangular ducts, *Int. J. Heat Mass Transfer* **10**, 1121–1123 (1967).
17. B. D. AGGARWALA, Bending of parallelogram plates, *J. Engng Mech. Div.* ASCE, **93**, No. EM4, Proc. paper 5373, pp. 9–18 (1967).
18. E. M. SPARROW, A. L. LOEFFLER and H. A. HUBBARD, Heat transfer to longitudinal laminar flow between cylinders, *Trans. Am. Soc. Mech. Engrs* (C), *J. Heat Transfer*, **83**, 415–422 (1961).

APPENDIX A

The Finite-Difference Approximation

A finite-difference procedure is described below. Although the general method is applicable to all the three geometries, details are given for the rhombic duct only.

From Fig. 10, because of symmetry, we need only to solve for W and T in one quadrant (say the 1st quadrant). The conditions to be applied

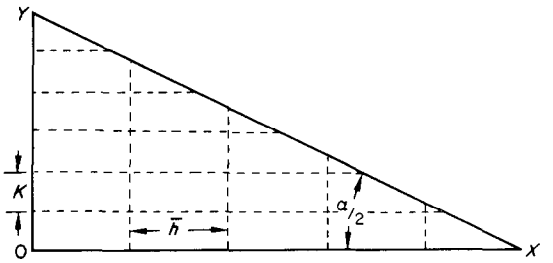

FIG. 10. Rectangular grid system for finite-difference procedure.

on the horizontal and vertical boundaries are that

$$\frac{\partial W}{\partial n} = \frac{\partial T}{\partial n} = 0,$$

where n is the normal to the appropriate edge. In order to avoid the problem of interpolation at the sloping boundary, a rectangular grid was used such that the horizontal step size

$$\bar{h} = \frac{X}{N} = \frac{1}{2N \sin a/2}, \qquad (A.1)$$

where N is the number of intervals along the X or Y axis.

The vertical step size

$$\bar{k} = \frac{Y}{N} = \frac{1}{2N \sin \alpha/2} = \bar{h} \tan \alpha/2. \qquad (A.2)$$

$$\text{Let } X_i = i\bar{h}, \qquad Y_i = j\bar{k}$$

and

$$W_{i,j} = W(X_i, Y_j), \qquad T_{i,k} = T(X_i, Y_j).$$

Then the standard 5-point approximation of the Laplacian at the point i, j, is

$$\nabla^2 T_{i,j} = \frac{1}{\bar{h}^2}\left\{T_{i+1,j} + T_{i-1,j} - 2T_{i,j}\right\} + \frac{1}{\bar{h}^2 \tan^2 \alpha/2}\left\{T_{i,j+1} + T_{i,j-1} - 2T_{i,j}\right\}. \quad \text{(A.3)}$$

Let

$$S_{i,j}T = T_{i+1,j} + T_{i-1,j} + \frac{1}{\tan \alpha/2}(T_{i,j+1} + T_{i,j-1}),$$

and let ω be the over-relaxation constant, then equations (7) and (8) become

$$W_{i,j} = \frac{\omega}{2(1 + 1/\tan \alpha/s)}\{\bar{h}^2(N_{Ra}W_{i,j} + E) + S_{i,j}T\} + (1 - \omega)\, W_{i,j}. \quad \text{(A.4)}$$

$$T_{ij} \frac{\omega}{2(1 + /\tan \alpha/2)}\{\bar{h}^2(F - W_{i,j}) + S_{i,j}T\} + (1 - \omega)\, T_{i,j}. \quad \text{(A.5)}$$

Now the algorithm proceeds as follows.

An initial distribution of W and T is assumed, as is a value of E. Then new values of W and T are calculated at each interior point of the grid using equations (A4) and (A5). (The points on the horizontal and vertical boundaries are calculated in a different manner which will be described shortly.)

Then W and T are re-calculated until on two consecutive iterations, the difference between the new and the old value of both W and T at every point differ in absolute value by not more than ε (usually $\varepsilon \approx 10^{-5}$).

Once the shape of W and T has "settled", the continuity equation (9) has to be checked. If it does not hold, then E has to be modified. Thus define

$$f(E) = \int_A W \,dX\,dY - \frac{1}{\sin \alpha}, \quad \text{(A.6)}$$

and E must be chosen so that $f(E) = 0$. A better value of E was determined using Newton's method for finding a zero of a non-linear equation, namely

$$E_l = E_{l-1} - \frac{f(E_{l-1})}{f'(E_{l-1})},$$

where l represents the iteration number.

After a new E is determined, W and T had to be "re-settled" as described above.

Still to be discussed is how the values are calculated for both W and T (on every iteration) along the horizontal and vertical boundaries. Using the forward-difference approximation for the derivative of a function at a point, one obtains

$$T_{i,j} = \tfrac{1}{3}(4T_{2,j} - T_{3,j}), \qquad j = 1, 2, \ldots N - 2,$$

for the points along the vertical boundary. Similar equations hold for T along the horizontal boundary and W along both the vertical and horizontal boundaries. The formula for the functions at the points (1, 1), (N, 1) and (1, N) have still to be given. It turns out that they are not needed during the "settling" of W and T and so need to be calculated only when E is being calculated. A simple average of the value of the function at the two nearest neighbours is used.

Comments

The practical problem of choosing an appropriate step size $\bar{h}$, an over-relaxation constant ω and the initial distribution of W and T remains to be discussed.

It was found that 50 intervals ($N = 50$) was about the minimum number required to guarantee an accurate shape for W and T. However, if the initial distribution of W and T were made zero, the number of iterations required

to "settle" the shape of W and T was prohibitive. Thus a value of $N = 20$ was first used to obtain a rough shape which was used as the initial distribution for the $N = 50$ case. A number of values of ω were tried, but $\omega = 1{\cdot}8$ seemed to be about the best.

With any value of ω between 1·0 and 1·9, the shape of the functions W and T were found to oscillate (as a function of the number of iterations). It was observed that when W was at an extremum, T had about the right (final) shape and vice versa. This fact was used to speed up convergence by saving the values of W when T was at an extremum, then when W was at an extremum, it was replaced by the previous saved values. This reduced the time for convergence by about a factor of 4. However, there still remains room for improvement in the methods used to further speed up convergence.

Table 1 presents sample values of the Nusselt number evaluated by the finite-difference method. In the same table, results of the variational formulation are also given for the sake of comparison.

APPENDIX B

In this Appendix, an exact solution of forced convection through a rhombic duct is presented.

For the case of pure forced convection ($N_{Ra} = 0$) and for $F = 0$ equations (7) and (8) reduce to

$$\nabla_1^2 W = -E, \tag{B.1}$$

$$\nabla_1^2 T - W = 0. \tag{B.2}$$

These combine into

$$\nabla^4 T = -E. \tag{B.3}$$

The boundary conditions for this case are

$$W = T = 0,$$

which are equivalent to

$$T = \nabla_1^2 T = 0 \tag{B.4}$$

at the boundary.

The problem posed by equations (B3) and (B4) is easily seen to be equivalent to the problem of deflection of a simply supported plate. Since the solution to this latter problem is available in the literature [17] for a parallelogram, we simply write down the expressions for velocity and temperature for the rhombic duct.

$$W = \frac{E}{4}\left[Z\bar{Z} - \lambda^2 \sum_1^\infty \sum_1^\infty \psi_p \psi_{p+n} \zeta^n - \lambda^2 \sum_1^\infty \sum_1^\infty \psi_p \psi_{p+n} \bar{\zeta}^n - \lambda^2 \sum_1^\infty \psi_n^2\right]^*, \tag{B.5}$$

and

$$T = \frac{-E\lambda^4}{16}\Bigg[Z^2\bar{Z}^2/4\lambda^4 - \tfrac{1}{4}\sum_1^\infty \sum_1^\infty \sum_1^\infty \sum_1^\infty \psi_r \psi_s \psi_p \psi_n \sigma^{|r+s-p-n|} e^{i(r+s-p-n)\phi} - \Bigg(\sum_1^\infty \sum_1^\infty \sum_1^\infty \sum_1^\infty \frac{r}{n+r} \psi_p \psi_{p+n} \psi_r \psi_s \zeta^{r+n} \bar{\zeta}^s + c \cdot c \Bigg) + \Bigg(\sum_1^\infty \sum_1^\infty \sum_1^\infty \sum_1^\infty \frac{r}{n+r} \psi_p \psi_{p+n} \psi_r \psi_s \times \sigma^{|n+r-s|} e^{i(+r-s)\phi} + c \cdot c \Bigg) - Z\bar{Z} \left(\sum_1^\infty \psi_n^2\right)/\lambda^2 + \left(\sum_1^\infty \psi_n^2\right)\left(\sum_1^\infty \sum_1^\infty \psi_r \psi_s \sigma^{|r-s|} e^{i(r-s)\phi}\right) \Bigg]. \tag{B.6}$$

Here the rhombus in ζ $(= X + iY)$ plane has been mapped onto a unit circle in the $\zeta(=\sigma e^{i\phi})$ plane, λ and ψ's are co-efficients of mapping,

$$Z = \lambda \sum_{n=1}^\infty \psi_n \zeta^n$$

is the mapping. Bar over a quantity and the letters c.c. denote "complex conjugate".

* Number of symbols required makes a certain amount of overlap in nomenclature unavoidable.

To compare the results obtained from (B5) and (B6) with the result obtained by the variational solution we present the values of W and T at the center of the duct by these two different methods, in Table 2. This table shows that the agreement between these two methods is very good.

Résumé—On étudie la convection mixte (naturelle et forcée) laminaire entièrement établie à travers des tuyaux verticaux à sections non-circulaires. Les géométries examinées sont les tuyaux dont la section est (i) un triangle rectangulaire, (ii) un triangle isocèle, et (iii) un losange.

On suppose soit que le flux de chaleur axial est uniforme soit que la température pariétale est uniforme le long du périmètre. Toutes les propriétés du fluide sont supposées constantes, sauf pour la variation de la masse volumique dans les termes de flottaison. Les solutions approchées du problème ont été obtenues par (i) le calcul des variations, (ii) le processus de differences finies.

Pour le tuyau losangique, on présente aussi une solution exacte pour la convection uniquement forcée. Pour le triangle rectangulaire, et pour $N_{Ra} = 0$, la valeur maximale du nombre de Nusselt est obtenue lorsque $\alpha = 45°$, tandis que, lorsque $N_{Ra} = 1000$, sa valeur minimale est obtenue lorsque $\alpha = 45°$. Pour le triangle isocèle, le nombre de Nusselt devient insensible également à l'angle du tuyau lorsque la valeur du nombre de Rayleigh augmente de zéro à environ deux mille. Lorsque le nombre de Rayleigh est encore augmenté jusqu'à dix mille, l'angle du tuyau devient de nouveau important. Pour le triangle isocèle, et pour $N_{Ra} = 0$, la valeur maximale du nombre de Nusselt est obtenue pour $\alpha = 60°$, tandis que, pour $N_{Ra} = 10000$, sa valeur maximale se présente pour $\alpha = 60°$. Pour le tuyau losangique, l'effet de l'angle du tuyau diminue lorsque la valeur du nombre de Rayleigh augmente à partir de zéro.

Zusammenfassung—Es wird eine vollausgebildete, laminare Strömung in senkrechten, nicht kreisförmigen Rohren behandelt, die durch kombinierte freie und erzwungene Konvektion bewirkt wird. Die behandelten Rohrquerschnitte sind: (i) rechtwinkeliges Dreieck, (ii) gleichschenkeliges Dreieck und (iii) Raute. Konstanter axialer Wärmefluss und am Umfang konstante Wandtemperatur werden angenommen. Alle Eigenschaften des Strömungsmediums werden als konstant betrachtet, mit Ausnahme veränderlicher Dichte in den Auftriebsgliedern Näherungslösungen des Problems werden durch Variationsrechnungen und mit Differenzenverfahren erhalten. Für rautenförmige Rohrquerschnitte wird bei rein erzwungener Konvektion auch eine exakte Lösung angegeben.

Für rechtwinklige Dreiecke hat der Rohrwinkel α keinen Einfluss auf die Nusselt–Zahl Nu, solange der Wert der Rayleigh–Zahl von 0 bis etwa 2000 ansteigt. Wird die Rayleigh–Zahl weiter erhöht, bis etwa 10000, so wächst der Einfluss des Rohrwinkels wieder. Für rechtwinkelige Dreiecke wird für $N_{Ra} = 0$ der grösste Wert der Nusselt–Zahl bei $\alpha = 45°$ erreicht, während sie für $N_{Ra} = 10000$ ihren niedrigsten Wert bei $\alpha = 45°$ hat. Für gleichschenkelige Dreiecke hat der Rohrwinkel ebenfalls keinen Einfluss auf die Nusselt–Zahl, wenn der Wert der Rayleigh–Zahl von 0 bis etwa 2000 steigt. Wird die Rayleigh–Zahl weiter erhöht, bis 10000, so erhöht sich der Einfluss des Rohrwinkels wieder. Für gleichschenkelige Dreiecke erhält man bei $N_{Ra} = 0$ den grössten Wert der Nusselt–Zahl für $\alpha = 60°$, während für $N_{Ra} = 10000$ ihr grösster Wert bei $\alpha = 90°$ liegt.

Für rautenförmige Rohrquerschnitte verschwindet der Einfluss des Rohrwinkels, wenn der Wert der Rayleigh–Zahl von Null ausgehend ansteigt.

Аннотация—Проведено исследование полностью развитого ламинарного течения при совместной свободной и вынужденной конвекции в вертикальном канале некруглого сечения. Рассматриваются каналы следующей геометрии поперечного сечения: прямоугольный треугольник, равнобедренный треугольник, ромб. Предполагается изотермичность стенок и однородность осевого теплового потока. Все свойства жидкости считаются постоянными за исключением плотности в членах подъемной силы. Приближенные решения получены с помощью (а) операционного исчисления и (б) методом конечных разностей. Для случая только вынужденной конвекции в ромбических каналах получено также точное решение. Для прямоугольного треугольника число Нуссельта (N_{Nu}) не зависит от угла канала (α), тогда как число Релея (N_{Ra}) повышается от 0 до 2000. При дальнейшем увеличении числа Релея, скажем, до 10000, угол канала опять начинает оказывать влияние. Для прямоугольного треугольника при $N_{Ra} = 0$ максимальное значение числа Нуссельта получается при $\alpha = 45°$. Для равнобедренного треугольника число Нуссельта опять перестает зависеть от угла канала при увеличении числа Релея от 0 до 2000. При дальнейшем росте числа Релея до 10000 угол канала опять становится важным фактором. Для равнобедренного треугольника при $N_{Ra} = 0$ максимальное значение числа Нуссельта получено при $\alpha = 60°$, тогда как при $N_{Ra} = 10000$ его максимальное значение соответствует $\alpha = 90°$. Для ромбических каналов влияние угла уменьшается при $N_{Ra} > 0$.